12. Fracture Toughness Evaluation of Low and Medium Strength Steels Based on the Stretched Zone

Akio OTSUKA,* *Member*, Takashi MIYATA,* *Member*,
Seiji NISHIMURA,* *Member* and Noboru KASAI**

(*From J.S.N.A. Japan, Vol. 136, Dec. 1974, Vol. 139, June 1976 and Vol. 142, Dec. 1977*)

Summary

Fracture toughness evaluation based on the deformation behavior at the precrack tip is discussed.

In part I it is shown that the stretched zone depth, as well as CTOD, is almost constant regardless of the test temperature when the crack initiates by fibrous crack, while, in cleavage initiation, it takes various values between the above-mentioned value and almost zero depending on the test temperature and plastic constraint. We call the value of CTOD at fibrous crack initiation δ_i (which is about the same value as 2(SZD) observed on the specimens in which the crack initiated by fibrous crack) and the fibrous-cleavage transition temperature in fracture initiation T_i. It is proposed to define the toughness of low and medium strength steels by two parameters δ_i and T_i.

In part II the effect of strain aging induced by preloading on toughness of steels has been investigated. The embrittling effect of this kind will be important in the case of preloading for stress relief or proof test, for instance. According to the test results, SS41 and SM41A show considerable amounts of embrittlement due to this type of strain aging, while in SM50C, the effect of aging is hardly observed.

Finally, in part III the effects of specimen thickness on T_i are investigated. T_i increases with increase in specimen size and takes upper limiting value (plane strain T_i) when plane strain state develops around the notch tip in the midthickness region. This situation is confirmed by the distribution of the stretched zone depth along the precrack front. Plane strain T_i may be assumed to be a material constant. As the specimen size requirement to give this plane strain T_i, the formula

$$a,\ B,\ W-a>0.4\frac{\delta_i E}{\sigma_Y R}$$

is proposed, where a is crack length, B specimen thickness, W specimen depth, δ_i COD at fibrous crack initiation, E Young's Modulus, σ_Y yield strength and R the ratio of yield strength to ultimate tensile strength.

Part I Fracture Toughness Evaluation by δ_i and T_i

1.1 Introduction

It has already been pointed out by several authors[1~4] that COD at the fibrous crack initiation is a good criterion for fracture initiation from a precrack. Some ambiguities, however, still seem to exist concerning the behavior of the "crack tip COD" (CTOD) during the fracture process.

In the present study, the deformation behavior of the precrack tip under the increasing load until fracture was investigated by microscopic observations by SEM.

* Nagoya University
** Kobe Steel Corp.

Table 1 Chemical compositions of steels

Steel	Thickness (as rolled) mm	Chemical compositions (%)									
		C	Si	Mn	P	S	Ni	Cr	Mo	V	N
A (JIS-SS41)	12	0.15	0.034	0.64	0.007	0.020	0.016	0.006	—	—	0.044
B (JIS-SS41)	22	0.12	0.22	0.39	0.011	0.030	—	—	—	—	—
C (JIS-SM41A)	25	0.17	0.017	1.14	0.017	0.017	0.021	0.022	0.004	—	0.0023
D (JIS-SM50C)	25	0.16	0.30	1.40	0.013	0.013	0.13	0.05	0.02	0.02	—
E (JIS-SM50C)	50	0.16	0.33	1.40	0.021	0.014	0.02	0.02	—	—	—
F (ASTM-A387B)	50	0.17	0.25	0.58	0.014	0.009	—	1.10	0.50	—	—
G (JIS-SM58Q)	50	0.13	0.42	1.02	0.013	0.005	0.17	0.01	0.25	0.014	—
H (HT80)	25	0.15	0.22	1.00	0.015	0.006	0.017	0.29	0.27	—	—

Table 2 Mechanical properties of steels

Steel	Yield strength kg/mm²	Tensile strength kg/mm²	Elongation %	Reduction of area %	V Charpy Test, $_{v}T_{rs}$ °C
A (JIS-SS41)	26.0	39.8	42.4	—	+5
B (JIS-SS41)	26.7	43.9	23.0	67.0	+12
C (JIS-SM41A)	23.6	46.7	42.7	73.4	−8
D (JIS-SM50C)	34.7	52.2	32.7	71.9	−38
E (JIS-SM50C)	35	54	36	—	—
F (ASTM-A387B)	36.1	55.9	36.4	77.5	−27
G (JIS-SM58Q)	50.0	60.7	30.8	76.4	−40
H (HT80)	77.7	82.9	19.6	70.8	−60

The stretched zone observed at the fatigue precrack tip of fractured specimen, firstly, noticed by Spitzig[5], is considered to be an important parameter which represents the behavior of the precrack tip of the specimen subjected to increasing load leading to fracture.[6~9]

In part I the variation of the stretched zone width with temperature was investigated with special attention to the fibrous-cleavage transition in fracture initiation. Then the toughness evaluation of low and medium strength steels based on the transition mentioned above was considered.

1.2 Materials, Specimens and Experimental Procedure

Chemical compositions and mechanical properties of steels used in the experiments are shown in Tables 1 and 2 (which also include the steels used in parts II and III). In Fig. 1 are shown the three-point bend specimens used in the tests. COD values measured by clip gages were converted to the crack tip values by using rotational fractor experimentally obtained for specimens of each size. Stretched zone width measured by SEM at 45° tilt angle was converted to stretched zone depth, which is denoted by 2(SZD) (see Fig. 10), by multi-

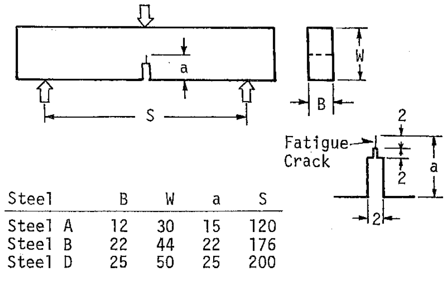

Fig. 1 Three-point bend specimens, dimensions in mm

plying $\sqrt{2}$. In parts II and III stretched zone depth was measured directly at 90° tilt angle as shown in Fig. 11 because this method proved to be more suitable to obtain the values of S.Z.D. than converting from S.Z.W., although the observation of SZW at 45° tilt is suitable for the observation of detailed structures of stretched zone.

1.3 Results and Discussion

(1) Stretched zone formation under increasing load

The stretched zone formation with increase in applied load was investigated by fracturing the specimens in liquid nitrogen after off-loading at various loads before fracture. An example of the stretched region of Steel A is shown in Fig. 2.

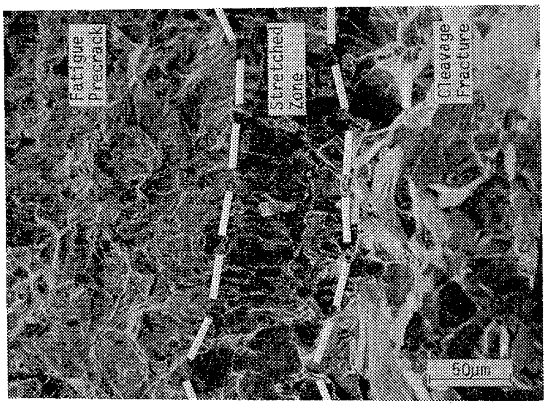

Fig. 2 An example of stretched zone, Steel A, −66°C

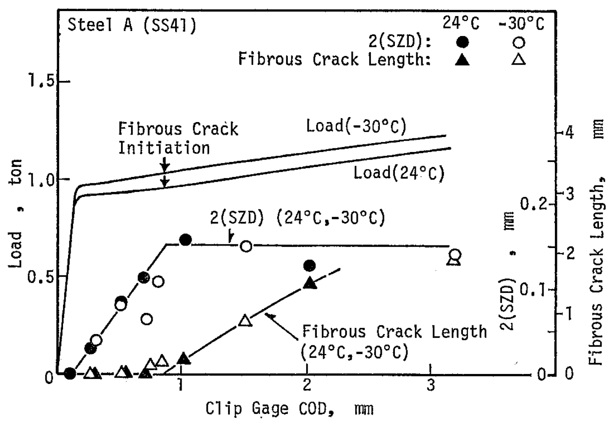

Fig. 3 Variation of load, stretched zone depth and fibrous crack length with clip gauge COD, Steel A, three-point bend test

Figure 3 shows loads, stretched zone depth and fibrous crack length as the function of clip gage COD at 24°C and −30°C. It is seen in this figure that the stretched zone is formed when COD attains to a certain value and that the size of the stretched zone increases with increase in COD until the size reaches a critical value at which fibrous crack initiates. After the initiation of fibrous crack, the size of the stretched zone does not change.

It is also interesting to notice that the relations between the stretched zone depth and COD are independent of temperature, and that their values at fibrous crack initiation are almost independent of temperature, too.

(2) Stretched zone depth as a function of test temperature

Because the stretched zone depth does not alter after the crack initiation as stated in the previous section, the stretched zone depth at the instant of fracture initiation can be measured on the fracture surface after the fracture tests. The stretched zone depths at the fracture initiation obtained by this method at various temperatures are shown in Figs. 4, 5 and 6, for Steels A, B and D, respectively.

It is seen that the notch tip behavior until fracture initiation is divided into three regions according to test temperatures, as shown in these figures. In the region 1 fracture occurs by fibrous crack with stretched zone; in the region 2 fracture occurs by cleavage with stretched zone; and in the region 3 by cleavage without stretched zone. It is evident from

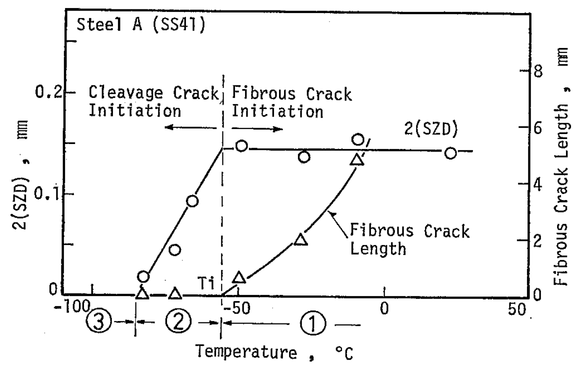

Fig. 4 Variation of stretched zone depth and fibrous crack length with temperature, Steel A, three-point bend test

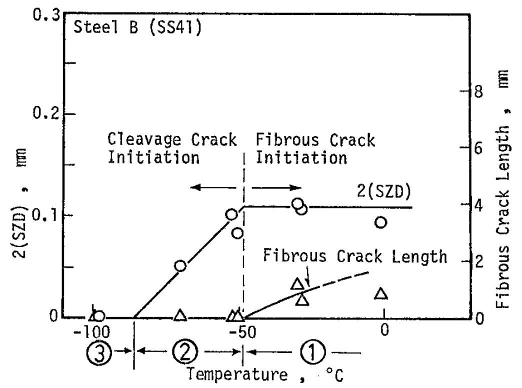

Fig. 5 Variation of stretched zone depth and fibrous crack length with temperature, Steel B, three-point bend test

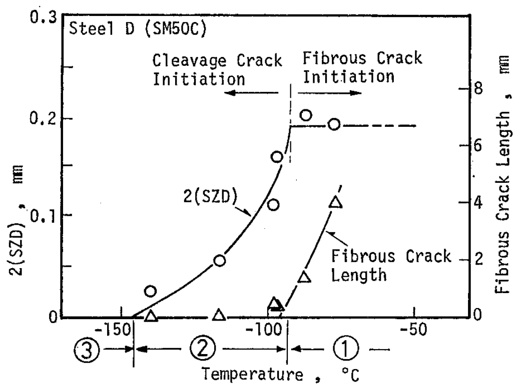

Fig. 6 Variation of stretched zone depth and fibrous crack length with temperature, Steel D, three-point bend test

these figures that in the region 1 the 2(SZD) is almost constant regardless of test temperatures and almost zero in the region 3, while in the region 2 it takes various values between the value in the region 1 and zero. In other words, the sizes of the stretched zone followed by fibrous crack are almost constant regardless of test temperatures, although those of the stretched zone followed by cleavage crack vary largely with test temperatures. It should also be noticed that the stretched zone depth in this case is affected not only by temperature but also by plastic constraint, because the temperature of the fibrous-cleavage transition in fracture initiation depends on plastic constraint.

Although the results on Steels A, B and D shown in Figs. 4, 5 and 6 show the similar situation, it is noticed that, some differences exist in the temperatures of the fibrous-cleavage transition at the crack initiation (T_i) and in the amounts 2(SZD) at which fibrous crack initiation occurs.

(3) Toughness criterion by δ_i and T_i

Figure 7 shows δ_c, 2(SZD), and fibrous crack length as a function of test temperature. It is noticed that δ_c shows very sharp change in the temperature range around T_i (fibrous-cleavage transition in fracture initiation), namely, if the temperature decreases toward T_i, δ_c decreases very sharply and, below T_i, it approaches almost zero. Another important point on fracture initiation behavior is that, at lower temperature than T_i, fracture initiation and unstable fracture occur simultaneously at CTOD$\simeq\delta_c$, and, at higher temperature than T_i, although fracture initiates at CTOD$\simeq\delta_i$, final fracture usually occurs at much larger value of δ, δ_c, as shown in Fig. 7, after some amount of stable crack growth.

Based on these characteristics of fracture initiation from a precrack, it seems to be reasonable to take the service temperature and service load of a steel structure so that they may be in the range of higher temperature than T_i and lower load than that at which CTOD reaches δ_i.

Accordingly, it would be also reasonable to define the toughness of steels by two parameters δ_i and T_i. Although it is already known that δ_i is almost constant independent of

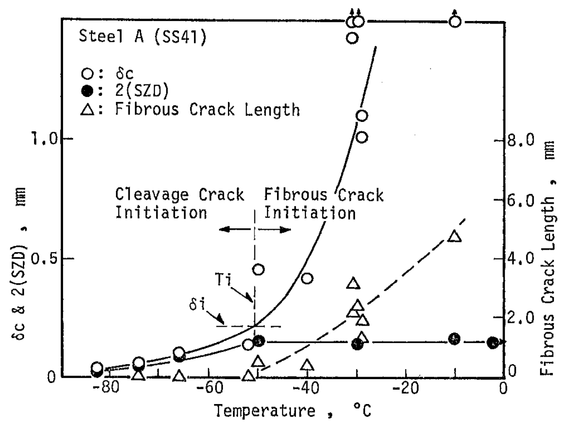

Fig. 7 CTOD at unstable fracture (δ_c) and stretched zone depth, 2(SZD), at various temperatures

various parameters, such as specimen size, test temperature, strain rate and so on, the characteristics of T_i is not so clear. On this problem, some investigation, will be made in part III in this paper.

It should be emphasized that, from the data on S.Z.D. as shown in Figs. 4~6, δ_i and T_i may be obtained as the value of 2(SZD) at fibrous crack initiation and as the transition temperature from region (1) to (2), respectively.

1.4 Conclusions

1. The stretched zone depth observed on the fracture surface 2(SZD) shows the crack tip COD (CTOD) at the fracture initiation.
2. In the case of fibrous crack initiation, the values of CTOD (δ_i) and 2(SZD) are almost constant regardless of test temperature, specimen geometries and other parameters.
3. In the case of cleavage fracture initiation CTOD and 2(SZD) take various values between the value at fibrous crack initiation (δ_i) and almost zero.
4. Toughness of steels will be defined by two parameters δ_i and T_i, where T_i is the fibrous-cleavage transition temperature in fracture initiation.

Part II Effects of Strain Aging Induced by Crack Tip Strain on Fracture Toughness

2.1 Introduction

The effect of strain aging induced by crack tip strain on toughness was investigated. If the steel which includes crack (or crack-like defect) is loaded to such a degree as to induce a stretched zone at the crack tip, the notch tip region will be embrittled by strain aging due to the large plastic strain around the stretched zone. This kind of embrittlement may occur, for instance, on preloading for stress relieving or proof test.

Tests were made on SS41, SM41A and SM50C. They were chosen for their variety of susceptibility of strain aging. Investigation was made under various amounts of preloading and at various aging time, with special attention to the behavior of crack tip deformation (stretched zone) leading to fracture initiation.

2.2 Materials and Specimens

Rimmed steel Steel A (SS41), usually with large aging effects, was mainly used in the experiment and, for comparison, killed steels Steels C and D (SM41A and SM50C) were also used. The chemical compositions and mechanical properties are shown in Tables 1 and 2, respectively. Although three-point bend specimens shown in Fig. 8(a) were mainly used, slow bend and impact tests were also made on Charpy-sized fatigue-cracked specimens shown by Fig. 8(b).

(a) Measurement of COD

Measurement of COD was made by the use of clip gage during all the tests except the

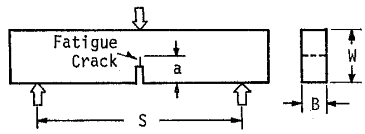

Steel	B	W	a	S
Steel A	12	30	15	120
Steel C	25	50	25	200
Steel D	10	30	15	120

(a) Three Point Bend Specimens

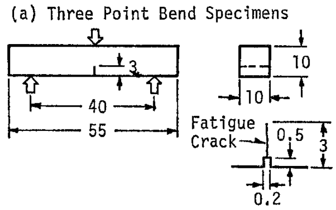

(b) Fatigue Cracked Charpy Specimens, Steel A

Fig. 8 Specimens, dimensions in mm

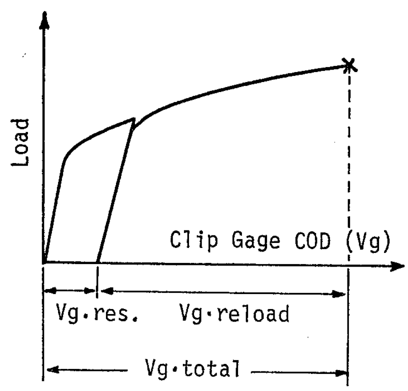

Fig. 9 Definitions of $V_{g,\mathrm{res.}}$, $V_{g,\mathrm{reload}}$ and $V_{g,\mathrm{total}}$

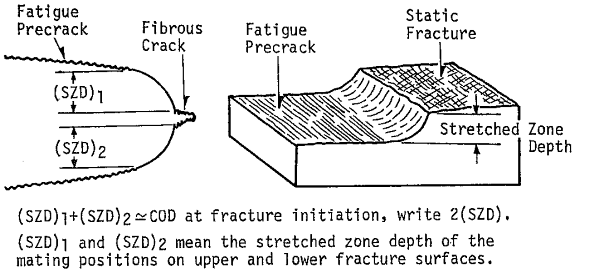

Fig. 10 Schematic illustration of the stretched zone

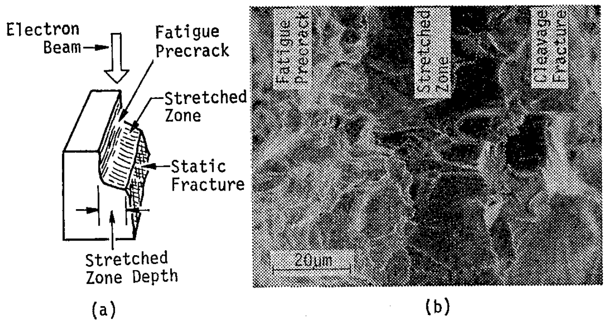

Fig. 11 Stretched zone. (a) Measurement of stretched zone depth by SEM, (b) An example of scanning electron micrograph of stretched zone, Steel A (SS41), preloaded (δ=0.1 mm), aged for 500 hours at +50°C, fractured at −30°C

impact tests. Measured values by clip gage (V_g) were converted to notch tip value (CTOD) by the use of rotational factor obtained by preliminary tests. The CTOD of the specimen preloaded and reloaded to fracture is obtained as shown in Fig. 9. Firstly, $V_{g,\mathrm{total}}=V_{g,\mathrm{res.}}+V_{g,\mathrm{reload}}$ (where $V_{g,\mathrm{res.}}$=residual V_g after preloading, $V_{g,\mathrm{reload}}$=increase in V_g during reloading) is made, then $V_{g,\mathrm{total}}$ is converted to crack tip value by the use of the curve of V_g~rotational factor.[10)]

Table 3 Aging conditions for each series of tests

Steel	Items investigated	Specimens	Amount of preloading	Aging (°C)—(hr)	Test temp. (°C)
SS41 (Steel A)	No aging No preload	Three-point bend (Fatigue cracked)	No preload (Fatigue-cracked)	20°C, <40 hr	−196~22
	Effect of aging time	〃	No preload (Fatigue-cracked)	20°C, 0~3000 hr	−30
			S.Z.D.≃40 μm (δ≃0.1 mm)	20°C, 0~3000 hr	−30
			〃	50°C, 0~1000 hr	−30
	Effect of amount of preloading	〃	No preload (Fatigue-cracked)	50°C, 63 hr	−70~−30
			S.Z.D.≃40 μm (δ≃0.1 mm)	〃 〃	−51~17
			δ≃0.27 mm (F.C.L.≃0.1~0.2 mm)	〃 〃	−50~10
			δ≃0.58 mm (F.C.L.≃0.7 mm)	〃 〃	−50~10
	Effect of aging in impact test	Fatigue cracked Charpy (Static and impact)	S.Z.D.≃30 μm	〃 〃	−90~95
SM41A (Steel C)	No aging No preload	Three-point bend (Fatigue cracked)	No preload (Fatigue-cracked)		−80~0
	Effect of aging after preloading	〃	S.Z.D.≃44 μm	50°C, 254 hr	−50~−10
SM50C (Steel D)	No aging No preload	〃	No preload (Fatigue-cracked)		−150~−70
	Effect of aging after preloading	〃	S.Z.D.≃40 μm	50°C, 63, 254 500, 100 hr	−90

(b) Measurement of SZD

Stretched zone is an important parameter which shows the notch tip behavior leading to fracture initiation. In Parts II and III stretched zone depth was measured in the way as shown in Figs. 10 and 11. The measurement was made at the points along the crack front on both upper and lower fracture surfaces at every 1 mm except 2 mm from both sides. An example of SEM photomicrograph is shown in Fig. 11.

(c) Experimental condition

Conditions of the experiments made in this study are shown in Table 3. On steel A (SS41), effects of aging time, amount of preloading and impact on toughness were investigated. The amouts of preloading were chosen so that a certain amount of stretched zone or fibrous crack may be induced at the precrack tip. The details of the conditions are given in Table 3.

In the case of steel C (SM41A), preloading was given by the amount to induce the stretched zone depth of 44 μm, and aging to 50°C for 254 hours. Tests were made in the temperature range which includes ductile-brittle transition.

In the case of steel D (SM50C), the amount of preloading is about the same as in SM41A (SZD$\simeq$40 μm), and aging times are 63, 254, 500 and 1000 hours. Test temperature was -90°C, which is a little higher than the T_i of the specimen with no preloading nor aging (-113°C). This temperature was chosen because it was expected that the effect of embrittlement would appear most pronouncedly around this temperature, if embrittlement occurs.

2.3 Results and Discussion

2.3.1 *Results on SS41*

(1) The effect of aging time on δ_c

In Figs. 12 (aged at 20°C) and 13 (aged at 50°C), the effect of aging time on critical COD (δ_c) is shown, where δ_c is the sum of $\delta_{res.}$ (residual COD after preloading) and $\delta_{c,\mathrm{reload}}$ (increase in COD during reloading to fracture). In Fig. 12, circular symbols and triangular symbols show the results of the unpreloaded specimens and those of preloaded ($\delta\simeq$0.1 mm) specimens, respectively. These data show that the toughness (δ_c) is reduced markedly by aging at 20°C for 1000 hours (Fig. 12) or at 50°C for 30 hours (Fig. 13). It is seen that δ_c's in these cases are sometimes almost zero.

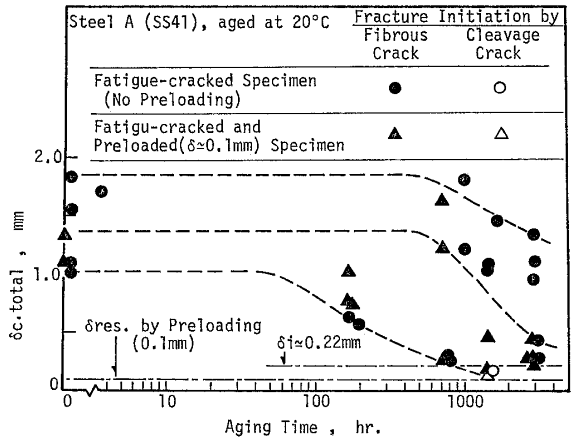

Fig. 12 Variation of $\delta_{c,\mathrm{total}}$ with aging time, Steel A, three-point bend specimen, aged at 20°C, test temperature -30°C

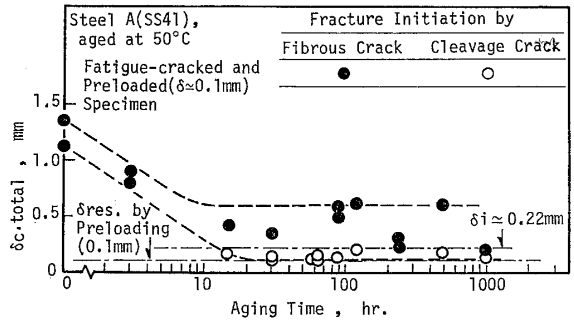

Fig. 13 Variation of $\delta_{c,\mathrm{total}}$ with aging time, Steel A, three-point bend specimen, aged at 50°C, test temperature -30°C

It should be noticed, however, that the very pronounced embrittling effect of aging shown in Figs. 12 and 13 is due to the fact that the test temperature chosen (-30°C) was between T_i's in unpreloaded and unaged condition (-50°C) and those in preloaded and aged condition (-20°C).

(2) The effect of aging time on fracture load

In Fig. 14 the fracture stress as a function of aging time is shown for the same specimen as shown in Fig. 13. Although the amount of the maximum reduction in fracture load

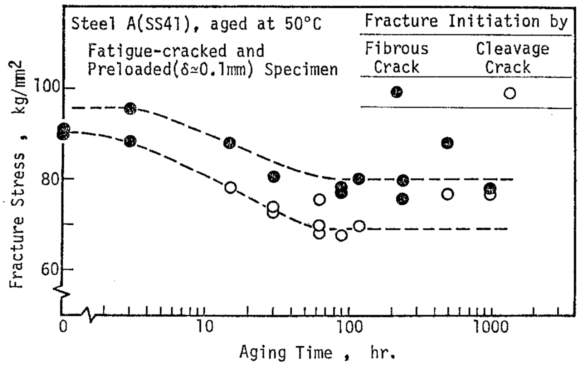

Fig. 14 Variation of nominal fracture stress with aging time, Steel A, three-point bend specimen, aged at 50°C, test temperature −30°C

induced by aging is about 20% in this case, it will be dependent on specimen size and geometry.

(3) The effect of aging on the test temperature $\sim \delta_c$ relation

Figure 15 shows the effects of the amounts of preloading on test temperature $\sim \delta_c$ relation for the specimens aged for 63 hours at 50°C. In this figure it is seen that appreciable increase in T_i is induced by the aging after preloading of $\delta \simeq 0.1$ mm (SZD$\simeq$40 μm), although the effect of aging is small when aged after fatigue precracking without preloading.

(4) Effect of strain aging in impact test

In this section, the embrittling effect of

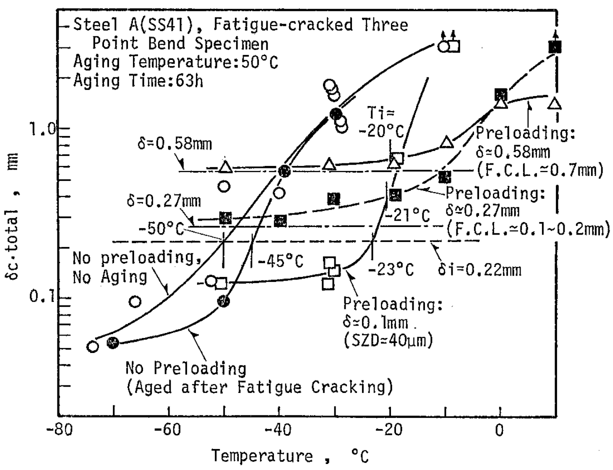

Fig. 15 Effect of the amount of preloading on the $\delta_{c,\mathrm{total}}$ at various temperatures, Steel A, fatigue-cracked three-point bend specimen, 50°C, 63 hours aged

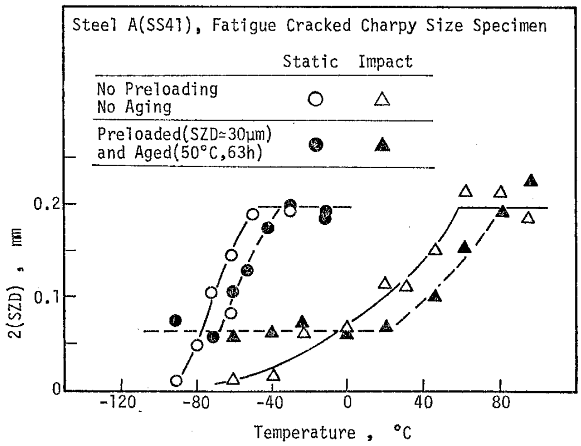

Fig. 16 Effect of the strain aging on 2(SZD) at various temperatures, Steel A, fatigue-cracked Charpy size specimen, static and impact test

strain aging in impact test was investigated, as the effect of aging may be larger in impact than in static as pointed out by Burdekin.[11] Tests were made both by impact and slow bend on fatigue-cracked Charpy-sized specimens.

As the toughness parameter, SZD was used for the comparison between the results of impact tests and those of static tests, because the measurement of COD in impact tests is not so easy as in static tests. The results are shown in Fig. 16. The conditions of aging are shown in Table 3 and also in Fig. 16.

From Fig. 16 it is realized that the effect of aging is larger in impact tests than in slow bend tests, but it is noticed that in this case the increase in T_i in slow bend test is about 10°C, which is much smaller than that shown in Fig. 15. This will be due to the effect of the specimen size. In other words, the ligament of the Charpy-sized specimen seems to be too small to evaluate the effect of embrittlement by aging.

Another interesting point shown in Fig. 16 is that the saturated values of 2(SZD) in both static and impact tests are the same ($\simeq$200 μm). They are also the same as the value in three-point bend test. The idea that δ_i will be a material constant has been confirmed in this case, too.

(5) $\delta_{c,\mathrm{total}} \sim 2$(SZD) relation

Figure 17 shows the relation between $\delta_{c,\mathrm{total}}$

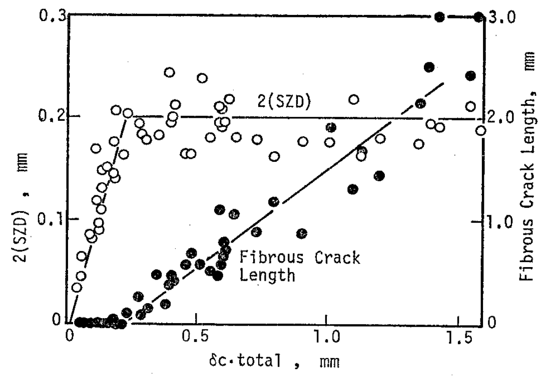

Fig. 17 2(SZD) and fibrous crack length versus $\delta_{c,\mathrm{total}}$ for various test conditions shown in Table 3, Steel A

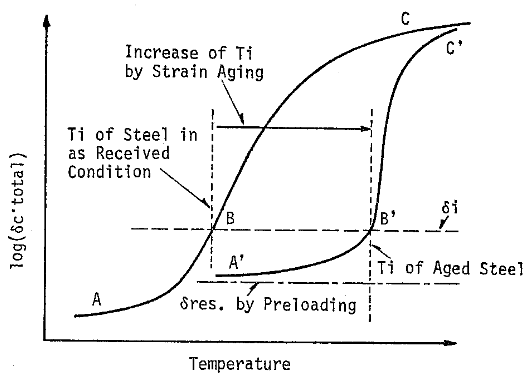

Fig. 19 Schematic illustration of the effect of strain aging on $\delta_{c,\mathrm{total}}$ at various temperatures

($\delta_{\mathrm{res}}+\delta_{c,\mathrm{reload}}$, where δ_{res}=residual δ after preloading, $\delta_{c,\mathrm{reload}}=\delta$ to fracture during reloading) and 2(SZD) in various experimental conditions. They include the data obtained by the tests made in the range of temperature $-196°\mathrm{C}\sim 20°\mathrm{C}$ under various amounts of preloading (fatigue precracking, stretched zone, stretched zone with fibrous crack) and after various aging time (0～1000 hours). It is noticed in this figure that 2(SZD) takes almost constant value in the range of $\delta_c>\delta_i$, ($\simeq$200 μm) independent of preloading, strain aging, or test temperature and, in the range of $\delta_c<\delta_i$, the relation between δ_c and 2(SZD) is almost linear (approximately 0.98 $\delta_c\simeq$2(SZD)).

2.3.2 *Results on SM41A*

In Fig. 18, the effect of strain aging is shown for the specimens preloaded to induce SZD of 44 μm and aged at 50°C for 254 hours. It is shown in this figure that T_i increased by about 17°C by strain aging.

This situation is schematically illustrated in Fig. 19. The effect of aging appears most pronouncedly where the test temperature is between the T_i in as-received condition (B) and that in aged condition (B′). At higher temperature than this (B′), δ_c in aged condition approaches to that in as-received condition very rapidly.

2.3.3 *Results on SM50C*

The results on SM50C are shown in Fig. 20. Tests on aged condition were made on

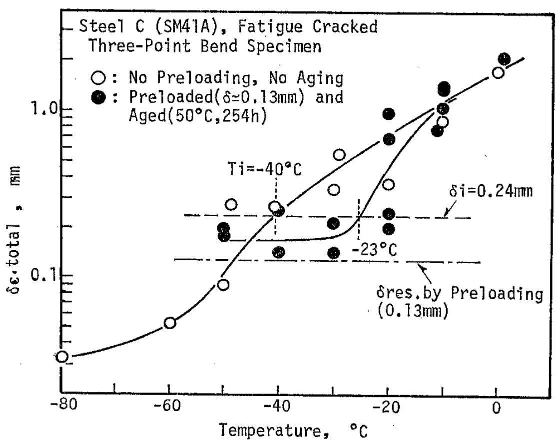

Fig. 18 Effect of strain aging on $\delta_{c,\mathrm{total}}$ at various temperature, Steel C, fatigue-cracked three-point bend specimen

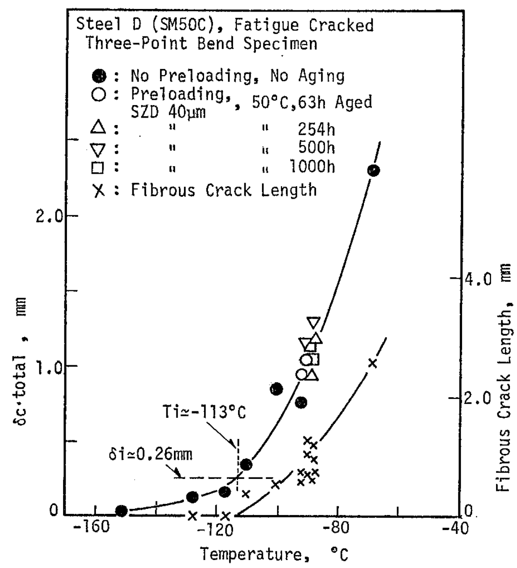

Fig. 20 Effect of strain aging on $\delta_{c,\mathrm{total}}$, Steel D, fatigue-cracked three-point bend specimen

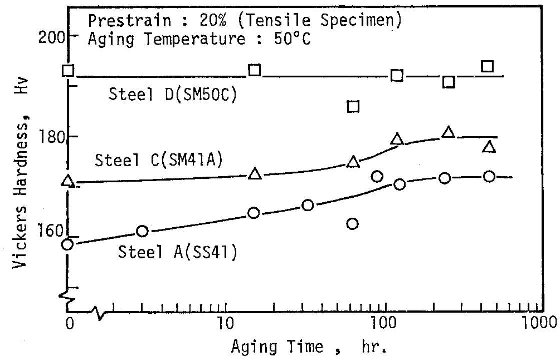

Fig. 21 Variation of the Vickers hardness of various steels (Steel A, C, D) strained 20%, with aging time, aging temperature: 50°C

the specimens preloaded to induce SZD of 40 μm and aged 63,254,500 and 1000 hours. Although the tests on specimens in as-received condition were made in the temperature range $-150°C \sim -60°C$, the tests in aged condition were made at $-90°C$, the temperature a little higher than T_i in the as-received condition ($-113°C$). This test temperature was selected so that δ_c may reflect the increase in T_i if any. In the results in Fig. 20, however, the effect of aging is hardly observed.

2.3.4 *Hardness Variations due to Strain Aging*

Hardness variations with aging time after plastic straining of 20% are shown in Fig. 21. According to this result, the hardening by strain aging is largest in SS41, and appreciable hardening is observed in SM41A, too, but no hardening is observed in SM50C. This tendency is almost similar to that of the embrittlement by strain aging. According to this result, the degree of the embrittlement by aging may be predicted by hardness test qualitatively.

2.4 Conclusions

Effects of the strain aging due to the strain around the crack tip on fracture toughness have been investigated for several structural steels. The main conclusions are as follows:

(1) Both of SS41 and SM41A show considerable amounts of embrittlement due to strain aging. The degree of embrittlement, however, is larger in SS41 (increase in T_i: 27°C) than in SM41A (increase in T_i: 17°C).

(2) This kind of embrittlement could occur in actual structures on preloading for stress relief or for proof test, for instance.

(3) In the case of SM50C no effect of aging was observed.

(4) The degree of hardening due to the strain aging shows similar tendency to that of the embrittlement of the same material, qualitatively.

Part III Effects of Specimen Thickness on T_i and Plane Strain T_i

3.1 Introduction

One problem when T_i and δ_i are used as toughness criteria is that, although δ_i may be regarded as a material constant,[1~4,12,13] T_i is not, but varies depending on various parameters such as specimen size, loading rate and so on. It is known that T_i increases with the increase in specimen size, and this is an important problem when we want to predict the behavior of actual structures from that of usual small specimens.

The increase in T_i with the increase in specimen size will be the results of the increased plastic constant (σ_{max}/τ_{max} of local stress in the notch tip region) due to the increase in thickness. If so, it will be quite natural to suppose that T_i will take the upper limiting value for the increase in specimen thickness (and other geometries) when the plane strain state develops at the notch tip region in the midthickness where fracture initiation occurs. This upper limiting value of T_i mentioned above (plane strain T_i) may be regarded as a material constant.

In part III, the dependence of T_i on specimen thickness and specimen size requirement to give the upper limiting value of T_i (or Plane Strain T_i) will be discussed.

3.2 Materials, Specimens and Experiment

Steel D (SM50C, 50 mm thick), Steel E (SM50C, 25 mm thick), Steel F (A387B), Steel G (SM58Q), and Steel H (HT80) shown Tables 1 and 2 were used. The fatigue-cracked,

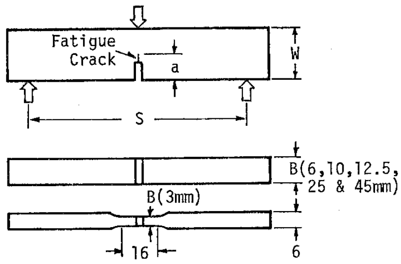

B	W	a	S
45	90	45	360
25	50	25	200
12.5	25	12.5	100
10	25	12.5	100
6	25	12.5	100
3	25	12.5	100

Fig. 22 Specimens, dimensions are in mm

three-point bend specimens used in this study are shown in Fig. 22. The specimens of reduced thickness were machined out of the part of the midthickness of the plate. Bend tests were made in the temperature range from low temperature where specimens show complete cleavage fracture to high temperature where specimens show fully ductile fracture. COD was measured by clip gage and it was converted to the crack tip value by the use of rotational factor which was obtained from the tests on each series of specimens in the same way as in parts I and II. After the fracture test, the stretched zone depth was measured by scanning electron microscope. The term 2(SZD) used in Figs. 24 and 28~31 denotes the sum of the S.Z.D.'s on the mating positions on the upper and lower fracture surfaces.

The measurement of the stretched zone depth by SEM was made to check the state of deformation (plane strain or plane stress) at the notch tip and also to check the values of δ_i obtained by clip gage and rotational factor.

3.3 Results and Discussion

(1) Fibrous crack initiation

Figure 23(a) and (b) show the examples of the relations between COD (at the original crack tip) and fibrous crack length of Steels A and B, respectively, for specimens of various sizes. It is seen in these figures that the relation between COD and fibrous crack length is independent of the specimen size, which means that δ_i (COD at fibrous crack initiation) is also

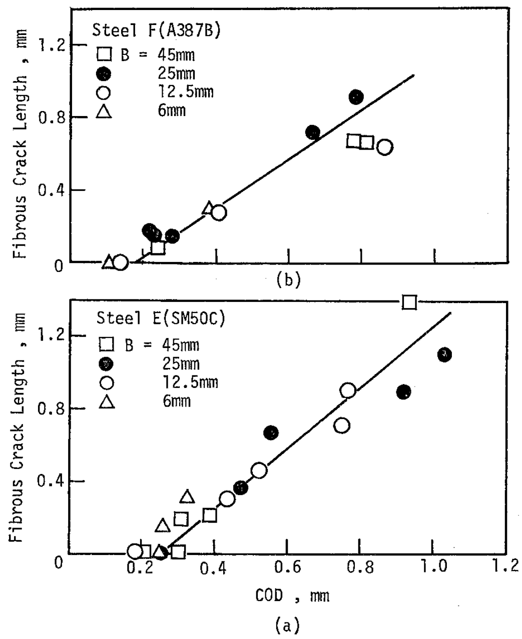

Fig. 23 COD versus fibrous crack length

independent of the specimen size. Such a behavior of COD is similar for other steels. In the case of 6 mm thick specimens of Steel A, however, the relation between COD and fibrous crack length shows the tendency to deviate slightly from other specimens.

The values of δ_i were checked by comparing with the values of 2(SZD). Figure 24 shows the distribution of 2(SZD) of the specimens in which the fracture initiation occurred by

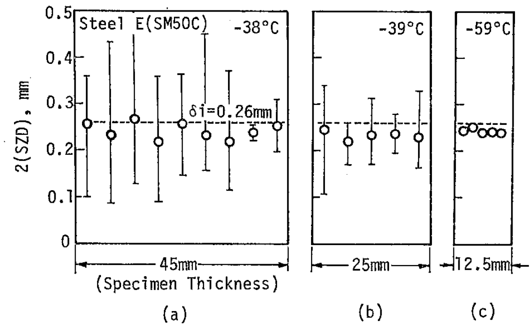

Fig. 24 Distribution of 2(SZD) along the crack front for Steel E. 2(SZD) is the sum of the S.Z.D.'s at the mating positions. (a) 45 mm thick specimen, fibrous crack length=1.45 mm, (b) 25 mm thick specimen, fibrous crack length=1.10 mm, (c) 12.5 mm thick specimen, fibrous crack length=0.9 mm

fibrous crack. It is noticed that the distribution of S.Z.D. is essentially uniform along the crack front and the value of 2(SZD) is very near to δ_i. All the δ_i's which were obtained by the method shown in Fig. 23 were checked by comparing with 2(SZD) observed on the specimens fractured with fibrous crack.

(2) Effect of specimen thickness on fibrous-cleavage transition temperature in fracture initiation (T_i)

In Figs. 25 and 26, some examples of the values of critical COD (δ_c, COD at unstable fracture, which occurred at the maximum load in the present series of tests) are shown for each steel. The temperatures at which $\delta_c=\delta_i$ in these figures are T_i's, where the fibrous-cleavage transitions in fracture initiation occurs.

The values of T_i obtained from the results of steels D~H, are plotted in Fig. 27 as the function of specimen thickness. It is seen in this figure that T_i generally increases with the increase in specimen thickness, although it is noticed that the effect of thickness on T_i is saturated for the specimens of Steel G thickner than 25 mm and the specimens of Steel H thicker than 10 mm. This behavior, T_i approaching the upper limiting value with the increase of specimen thickness, will correspond to the event that plastic constraint approaches the maximum value as the result of the development of plane strain condition at the notch root in the midthickness region, where crack initiates. To confirm this view, the deformation around the notch tip was examined by measuring the distribution of the S.Z.D. along the crack front.

Figures 28~31 show the distribution of the S.Z.D. of the specimens of various thickness

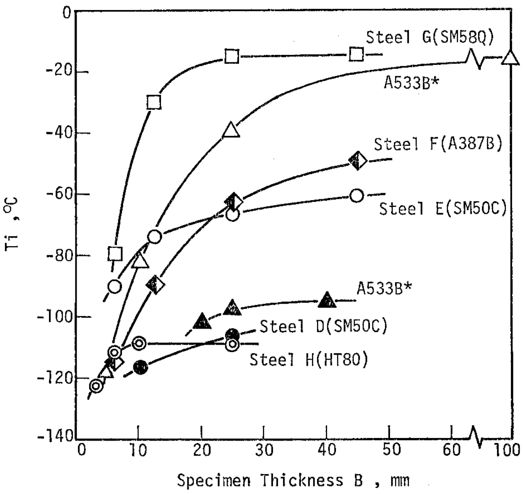

Fig. 27 Variation of T_i with specimen thickness for various steels, * Data from ref. 17

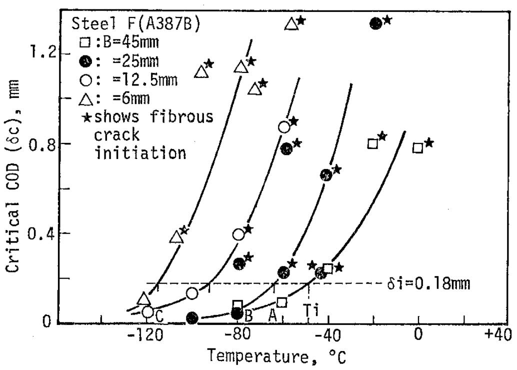

Fig. 25 Variation of critical COD with temperature, Steel F

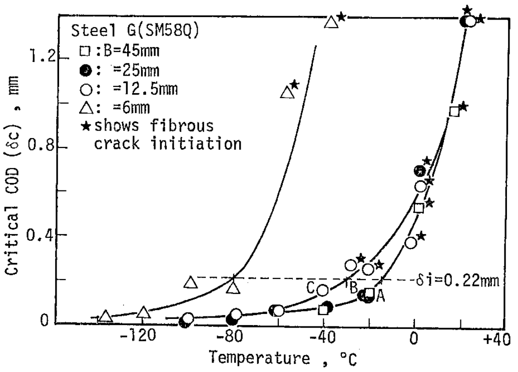

Fig. 26 Variation of critical COD with temperature, Steel G

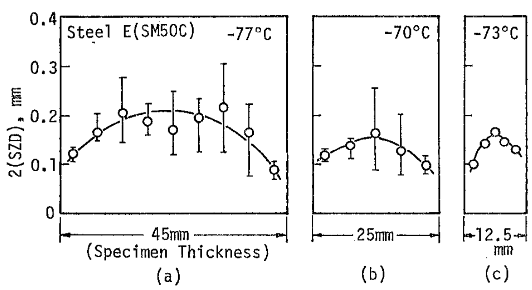

Fig. 28 Distribution of 2(SZD) along the crack front for Steel E. (a) 45 mm thick specimen, (b) 25 mm thick specimen, (c) 12.5 mm thick specimen

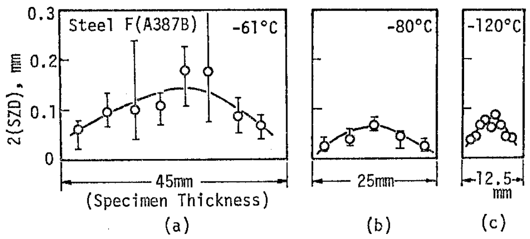

Fig. 29 Distribution of 2(SZD) along the crack front for Steel F. The specimens shown in figures (a), (b) and (c) are indicated in Fig. 25 by the letters A, B and C, respectively. (a) 45 mm thick specimen, (b) 25 mm thick specimen, (c) 12.5 mm thick specimen

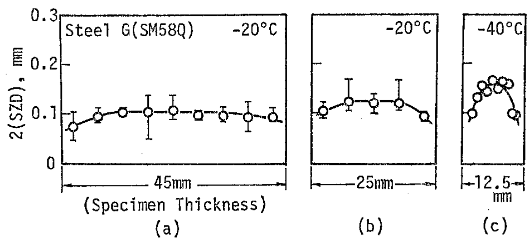

Fig. 30 Distribution of 2(SZD) along the crack front for Steel G. The specimens shown in figures (a), (b) and (c) are indicated in Fig. 26 by the letters A, B and C, respectively. (a) 45 mm thick specimen, (b) 25 mm thick specimen, (c) 12.5 mm thick specimen

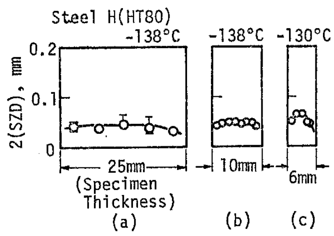

Fig. 31 Distribution of 2(SZD) along the crack front for Steel H. (a) 25 mm thick specimen, (b) 10 mm thick specimen, (c) 6 mm thick specimen

for Steel E, F, G and H fractured below the temperature T_i. If we compare Fig. 27 with Figs. 28~31, it will be noticed that the S.Z.D. of the specimens, of which T_i takes the saturated value, shows flat distribution in the region around the midthickness as will be seen in the case of 25 mm thick and 45 mm thick specimens of Steel G (Fig. 30) and 10 mm thick and 25 mm thick specimens of Steel H (Fig. 31), while in the case of other specimens the S.Z.D. shows convex parabolic distribution and there is no region of flat distribution. From these observations it will be reasonable to suppose, that if the plane strain condition develops at the notch tip in the midthickness region, T_i takes saturated value, and that, in the case where the plastic constraint is lower than this state, T_i shows thickness dependence and S.Z.D. takes convex distribution.

(3) Upper limiting value of T_i, plane strain T_i

To obtain this saturated value of T_i by experiment, it would be desirable if the specimen size requirement to obtain plane strain T_i be given. If we take the parameter $\delta_i E/\sigma_Y BR$ as the abcissa and take the value of T_i as the ordinate, the test results show the behavior as shown in Fig. 32. E is Young's modulus, σ_Y yield strength, B specimen thickness and R the ratio of yield strength to ultimate tensile strength at the temperature T_i.

In the present study, the phenomenon of saturation in T_i is observed on Steels G and H. Then, from Fig. 14, it may be suggested, though not conclusively, that in the region

$$\delta_i E/\sigma_Y BR < 2 \sim 4 \tag{1}$$

T_i takes the saturated value.

As the specimen sizes are varied proportionally in the present study (although there

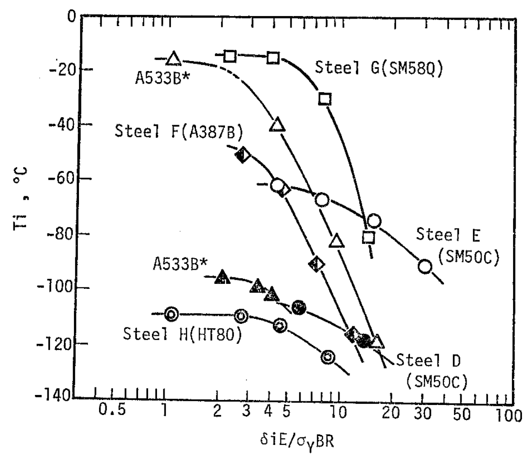

Fig. 32 Variation of T_i with a parameter $\delta_i E/\sigma_Y BR$, * Data from ref. 17

are some exception), it would be appropriate to suppose that the specimen size requirement for plane strain T_i will be given by the following formula,

$$a,B,W-a>0.4\frac{\delta_i E}{\sigma_Y R} \qquad (2)$$

where a is crack length and W is specimen depth.

If we write eq (2) in terms of J_i (values of J at the initiation of slow tearing) instead of δ_i, the following equation is to be obtained, by using the relation $J=\lambda\sigma_Y\delta$[14]

$$a,B,W-a>\frac{0.4}{\lambda}\frac{J_i E}{\sigma_Y{}^2 R} \qquad (3)$$

where according to Robinson[15], $\lambda=1$ for En 24 Steel ($\sigma_Y=1025\,\mathrm{MN/m^2}$) and $\lambda=2.6$ for En 32 Steel ($\sigma_Y=275\,\mathrm{MN/m^2}$). If T_i is obtained on the specimens which satisfy the conditions of (2) or (3), it will be the upper limit of T_i (plane strain T_i). It means that, at higher temperature than this fracture initiation from a precrack always occurs by fibrous crack regardless of the specimen size and geometry. This plane strain T_i is supposed to be a material constant.

As Sumpter[16] suggested recently, the geometry independence of J_i (as well as δ_i) is justified only for the case of failure by microvoid coalescence (fibrous fracture). It is obvious, according to the above discussion, that this requirement of microvoid coalescence will be satisfied for specimens of any size, including a very large one which simulate actual structures, if the temperature is higher than plane strain T_i.

For the safety of the structures in service from unstable fracture, it is important to know to what extent the temperature T_i will increase due to the plastic constraint of the structure which is supposed to be much higher than that of usual small specimens. For this purpose it will be reasonable to use the upper limiting value of T_i (plane strain T_i) mentioned above.

From the argument made above, it may be said that the lowest service temperature of a steel structure should be higher than plane strain T_i of the steel used, and the service load should be smaller than the load at which CTOD attains δ_i.

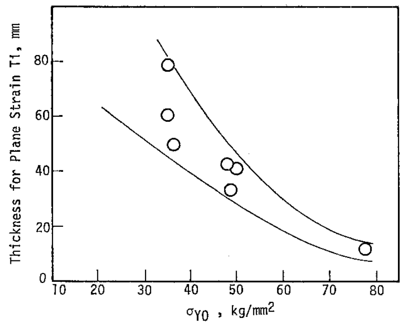

Fig. 33 Estimated thickness for plane strain T_i from eq. (2)

The specimen thickness required to give the plane strain T_i is given as shown in Fig. 33, by plotting the relation between B and σ_Y using the value of δ_i and R of the steels used in this study.

3.4 Conclusions

The effects of specimen size on the transition in fracture toughness of low and medium strength steels have been investigated. Main conclusion are as follows:

(1) T_i generally increases with the increase in specimen thickness but shows the tendency to approach some limiting value.

(2) This limiting value of T_i (plane strain T_i) is attained when the plastic constraint at the notch tip region in the midthickness reaches the plane strain condition, which was confirmed from the distribution of S.Z.D. along the crack front. This limiting value of T_i (plane strain T_i) will be a material constant.

(3) From the view of the safety of the steel structure, the lowest service temperature should be higher than plane strain T_i of the steel used, and the service load should be smaller than the load at which CTOD attains δ_i.

(4) The specimen size requirement to give plane strain T_i may be given by the following formula.

$$a,B,W-a>0.4\frac{\delta_i E}{\sigma_Y R}$$

Acknowledgement

The authors would like to thank Mr. T. Yamada (now at Mutsumi Industrial Co.) for his assistance in experimental work.

References

1) P. Terry and J.T. Barnby; Determining Critical Crack Opening Displacement for the Onset of Slow Tearing in Steels, Metal Const. and Brit. W.J., Vol. 3 (1971). pp. 343–345
2) G.D. Fearnehough, G.M. Lees, J.M. Lowes and R.T. Weiner; The Role of Stable Ductile Crack Growth in the Failure of Structures, *Practical Application of Fracture Mechanics to Pressure Vessel Technology*, (1971) pp. 119–128
3) R.F. Smith and J.F. Knott; Crack Opening Displacement and Fibrous Fracture in Mild Steel, ibid., pp. 65–75
4) C.G. Chipperfield, J.F. Knott and R.F. Smith; Critical Crack Opening Displacement in Low Carbon Steels, Conf. Book of the 3rd Int. Conf. Fracture, Munich, (1973) Teil II, I-233
5) W.A. Spitzig; A Fractographic Feature of Plane-Strain Fracture in 0.45 C-Ni-Cr-Mo Steel, Trans. ASM, Vol. 61 (1968) pp. 344–349
6) J.P. Tanaka, C.A. Pampillo and J.R. Low, Jr.; Fractographic Analysis of the Low Energy Fracture of an Aluminum Alloy, ASTM STP 463 (1970) pp. 191–215
7) K. Schwalbe; Processes at the Tip of a Crack under Continuously Increasing Loads, Conf. Book of the 3rd Int. Conf. Fracture, Munich, (1973) Teil IV, III-515
8) D. Elliott; Crack Tip Processes Leading to Fracture, *The Practical Implications of Fracture Mechanisms*, The Institution of Metallurgists, (1973) pp. 21–27
9) D. Broek; Correlation between Stretched Zone Size and Fracture Toughness, Eng. Frac. Mech., Vol. 6 (1974) pp. 173–181
10) J.F. Knott; *Fundamentals of Fracture Mechanics*, Butterworths (1974), p. 157
11) F.M. Burdekin; Fracture Testing of Weldments in Structural Steels, Brit. Welding J., Vol. 15 (1968) pp. 268–275
12) A. Otsuka and T. Miyata; Effects of Plastic Constraint on the Fracture Mode and COD, *Significance of Defects in Welded Structures ed. by T. Kanazawa and A.S. Kobayashi, Univ. of Tokyo Press*, (1974) pp. 292–307
13) S. Kanazawa, K. Minami, K. Miya, S. Sato and I. Soya; An Investigation of Static COD and Dynamic COD, J. Soc. Nav. Arch. Japan, Vol. 133 (1973), pp. 257–265 (in Japanese)
14) D.J. Hayes and C.E. Turner; An Application of Finite Element Techniques to Post-Yield Analysis of Proppsed Standard Three-Point Bend Fracture Test Pieces, Int. Journal of Fracture, Vol. 10 (1974), pp. 17–32
15) J.N. Robinson; An Experimental Investigation of the Effect of Specimen Type on the Crack Tip Opening Displacement and J-Integral Fracture Criteria, Int. Jour. Fracture, Vol. 12, No. 5 (1976), pp. 723–737
16) J.D.G. Sumpter; The Prediction of K_{IC} using J and COD from Small Specimen Tests, Metal Science, Vol. 10, October (1976), pp. 354–356
17) Doc. JI-No. 57, JI-No. 73, JI-No. 74 (1977), Committee-JI, Japan Weld. Eng. Soc.